sciendo

LATVIAN JOURNAL OF PHYSICS
AND TECHNICAL SCIENCES
2019, N 3

DOI: 10.2478/lpts-2019-0019

ENGINEERING AND TECHNOLOGY

LOW-COST L-BAND RECEIVING SYSTEM FRONT-END FOR IRBENE RT-32 CASSEGRAIN RADIO TELESCOPE

M. Bleiders*, A. Berzins, N. Jekabsons, K. Skirmante, Vl. Bezrukovs
Engineering Research Institute "Ventspils International Radio Astronomy Center",
Ventspils University College, Inzenieru Str. 101, Ventspils, LV-3601, LATVIA
*e-mail: marcis.bleiders@venta.lv

Irbene RT-32 radio telescope is one of the main instruments operated by Ventspils International Radio Astronomy Center (VIRAC), which is used for participation in VLBI and single-dish mode observations, including European VLBI Network (EVN) and other astronomy projects such as recently started research on small bodies of solar system, which involves weak spectral line detection at L-band. Since start of the operation as a radio telescope, single C-X band receiver has been available at RT-32, but regular demand for L-band frequencies has been received due to its importance in spectral line science. In case of RT-32 geometry, optimum dimensions of L-band feed antenna system are inconveniently large and its installation without significant feed cone rebuilding is complicated. While work is currently ongoing to redesign the feed cone for multiple receiver support and to develop high performance L-band feed system, temporal, compact and low-cost receiver has been built and installed laterally to secondary focus, which in sense of performance and functionality has been proven to be appropriate for most of the current needs. Receiver is based on small parabolic reflector allowing one to use a compact dual circular polarized horn antenna, which together with a Cassegrain antenna forms a three-mirror system. Front-end is uncooled that allows reducing operational and maintenance costs, while still providing acceptable noise performance. Practical tests show average overall sensitivity of 750 Jy at 1650 MHz in terms of system effective flux density (*SEFD*). The paper describes the development of the receiver and presents the main results of performance characterization obtained at Irbene RT-32.

Keywords: *feed antenna, radio telescope, receiver*

1. INTRODUCTION

RT-32 originally was built as a satellite communications station. Only in recent years it has been refurbished to function as a radio telescope. Its secondary focus vertex room is intended for a single receiver feed system and currently a

cryogenic C-X band receiver is installed there. There were attempts to implement L-band receivers in existing RT-32 system based on a helical antenna array as a feed antenna [1], [2], but due to specific application of satellite signal reception, its performance specification was less constrained; as a result, sensitivity of these designs were not sufficient for astronomy involving natural sources. In addition, due to a feed solution, only a single polarization channel was available and manual installation of receiver before observation was required which increased maintenance cost, decreased frequency band agility, and complicated the calibration. To deal with these issues, a receiving system was redesigned, by employing a compact feed antenna permanently installed at secondary focus with lateral offset, uncooled low noise amplifiers and improved frequency conversion and control unit. The following sections of the paper describe the design process of the above-mentioned subsystems and summarise the main results of performance evaluation.

2. THE REQUIRED DIMENSIONS OF FEED ANTENNA

In case of RT-32 geometry, its Cassegrain ratio of focal length to diameter at secondary focus is $f/D = 2.7$, which translates to a secondary mirror subtended angle of $\theta = 21^{\circ}$. As an initial design specification, a rule-of-thumb required an illumination pattern edge taper of 10 to 13 dB. Design frequency is set to 1650 MHz, which is at the centre of frequency band usually observed by EVN. To obtain an idea of necessary optimum dimensions of feed antenna, first, we calculate ideal case corrugated feed horn dimensions by approximating the telescope as a quasi-optical system where feed horn must generate appropriate a Gaussian beam waist at focal position. Radius of beam waist can be calculated in terms of illuminated mirror effective ratio f/D and required edge taper [3, 6.68b]:

$$W_0 = 0.216\sqrt{|T(dB)|}\frac{f}{D}\lambda\,. \tag{1}$$

T is edge taper in dB. In case of RT-32, $W_0 = 0.34$ m is obtained at 1650 MHz and edge taper of 10 dB. For practical horn, a quadratic phase error of between the centre and edge of the aperture must be finite and here a phase error of $\beta = 1.26$ rad (0.2λ) is assumed. This allows finding corrugated feed horn aperture radius and slant length which maximizes coupling to a fundamental Gaussian beam mode [3], [4]:

$$a = W_0\frac{\sqrt{1+0.172\beta^2}}{0.644}\,, \tag{2}$$

$$L = \frac{\pi a^2}{\lambda\beta}\,. \tag{3}$$

Using (2) and (3), dimensions of aperture diameter and slant length of the hypothetical corrugated horn can be found: $D_\alpha = 2\alpha \approx 1.17$ m and $L \approx 4.7$ m, respectively. It is the large length, which is currently practically inconvenient in case of RT-32, so as a temporal solution, feed aperture is approximated by replacing the full-size horn with the third focusing reflector to reduce the final beam waist, thus allowing one to reduce dimensions of the required feed significantly. Similar approach has been reported in [5]. Standard size parabolic reflector with $D = 1.2$ m and ratio $f/D = 0.4$ (subtended angle $\theta = 128^\circ$) is used, which matches good with the previously calculated required aperture diameter D_α.

3. FEED HORN FOR ILLUMINATING THE THIRD REFLECTOR

Feed horn design was adapted from [6] and scaled to 1650 MHz. This horn consists of a single mode circular waveguide and /4 choke ring to suppress the sidelobes while its relatively small size reduces reflector blockage. Dual circular polarizations are obtained using a septum polarizer, which also serves to separate orthogonal modes. Before manufacturing, the feed horn was modelled and optimized for the best return loss with practical metal part thicknesses using CST MWO. Waveguide to coaxial transitions was also included in simulation. Simulated far fields are shown in Fig. 1, while Fig. 5 demonstrates simulated and measured S parameters.

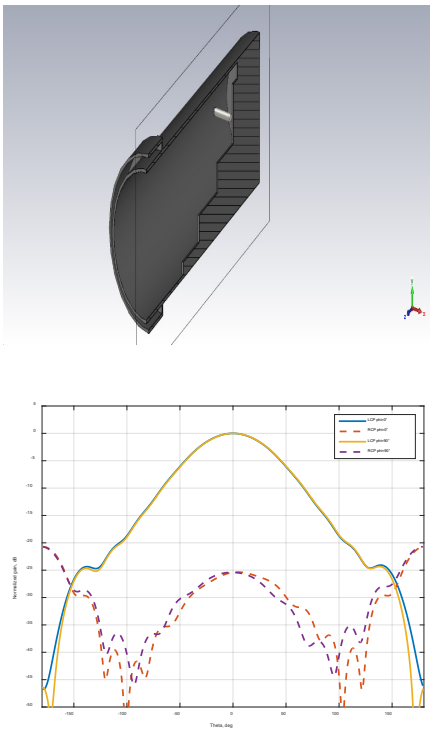

Fig. 1. (Left) Cutting plane of 3D model of feed horn in CST. (Right) Simulated far field RCP and LCP beam patterns at Phi cuts of 0º and 90º.

The main dimensions of final optimized feed horn at 1650 MHz are the following: D_α = 132 mm, L = 393 mm, Thickness of septum: 5 mm. As follows from Fig. 1, the same beam width at both Phi planes with a cross-polar level of 25 dB is obtained. Amplitude taper at beam angle of θ = 128º is ≈ 9.4 dB.

4. MODELLING OF REFLECTOR SYSTEM

As the first step, the system consisting of feed horn and 1.2 m parabolic reflector is analysed in CST and the obtained far-field beam patterns are shown in Fig. 2. Feed support metal tripod was also included in simulation. Unfortunately, blocked, electrically small aperture gives rise to relatively large sidelobes, which are non-symmetric due to feed supports. Offset reflector would reduce aperture blockage, but at the cost of increased overall dimensions. Cross-polarization level of feed horn antenna is preserved relatively well. Amplitude taper of the obtained pattern at RT-32 secondary mirror subtended angle of 21º is about 17 dB, which is larger (beam is narrower) than predicted when radiating aperture is corrugated horn with the same diameter.

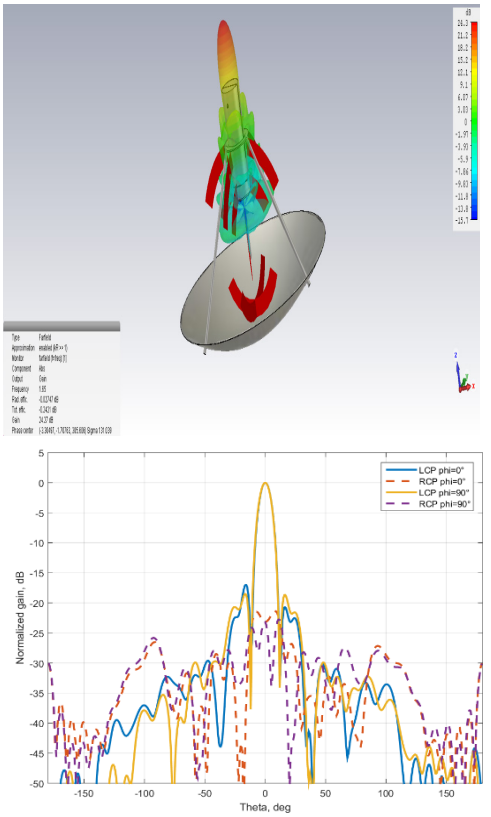

Fig. 2. (Left) 3D model of composite feed – 1.2 m third reflector and compact horn. Red area shows the position of far-field phase centre of the whole structure. (Right) Simulated far-field RCP and LCP beam patterns at Phi cuts of 0º and 90º.

Next, simple modelling of overall performance was performed using physical optics code based on [7]. Ideally aligned and appropriately meshed RT-32 Cassegrain reflector surfaces were assumed without considering the influence of the secondary mirror support leg. Far-field pattern shown in Fig. 2 was used as an illuminating point source – although distance between the source point and the first reflector is smaller than Fraunhofer distance of composite feed, results should still give a rough estimate of overall performance. Resulting boresight region beam patterns with composite feed offset and orientation angle relative to centre axis at secondary focus of 1 m and 8º, respectively, are shown in Fig. 3.

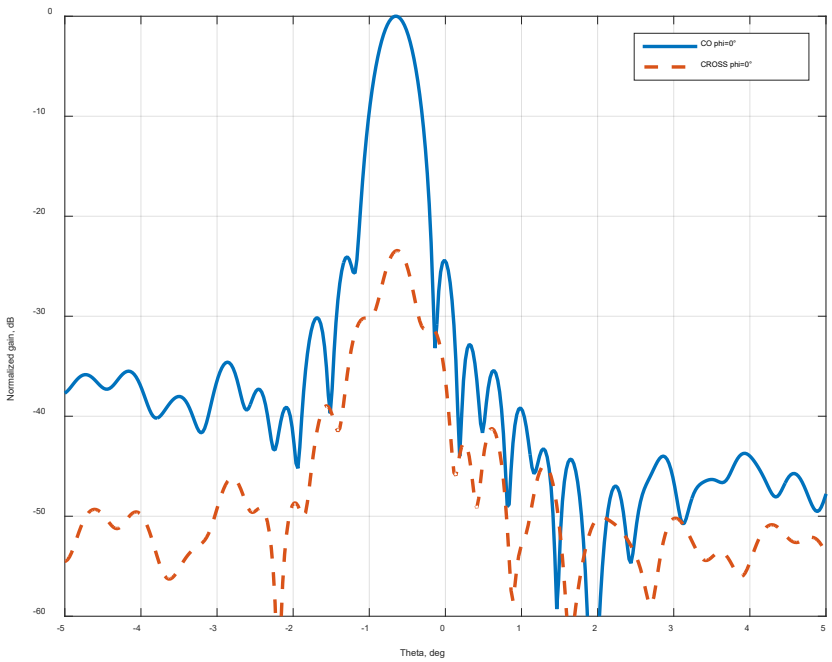

Fig. 3. Physical optics result of overall RT-32 co-polar and cross-polar beam pattern with a laterally shifted composite feed antenna. Pattern cut angle matches with lateral shift plane.

Maximum directivity of 52.3 dBi is calculated, which corresponds to aperture efficiency e_P = 0.55. As mentioned previously, an ideal reflector system was assumed. In the real world, efficiency would be degraded due to additional factors. It is estimated from photogrammetric measurements that RMS error of RT-32 primary surface is ≈4 mm, which translates to surface efficiency e_S = 0.9 at 1650 MHz according to Ruze. It is known from beam pattern measurements at C-band that the secondary mirror of RT-32 is misaligned – the assumed degradation at L-band is e_M = 0.9. Additional factor e_R = 0.9 is assumed due to secondary mirror support leg diffraction and imperfections of practical implementation. This would result in expected overall aperture efficiency not more than $e_A \approx e_P e_S e_M e_R$ = 40 %. Physical optics result also shows the main beam offset angle of -0.66º, which is opposite to lateral shift direction. The predicted cross-polarization level is 23 dB.

5. FEED ANTENNA INSTALLATION AT RT-32

Composite feed antenna was built and installed at RT-32 secondary focus with phase centre lateral offset of 1 m and angle of 8º as shown in Fig. 4. Before installation, S parameters of feed horn separately were measured with waveguide opening facing clear sky. Attempt was made to experimentally trim length of coaxial to waveguide interface monopole antennas to further optimize return loss, but no significant improvement was observed relative to dimensions predicted by CST. Measurement results show return loss better than 15 dB within the frequency range from 1450 to 1720 MHz (see Fig. 5). The measured port-to-port isolation is ≈18 dB at 1650 MHz.

Fig. 4. L-band feed antenna installed at RT-32 with offset from secondary focus.

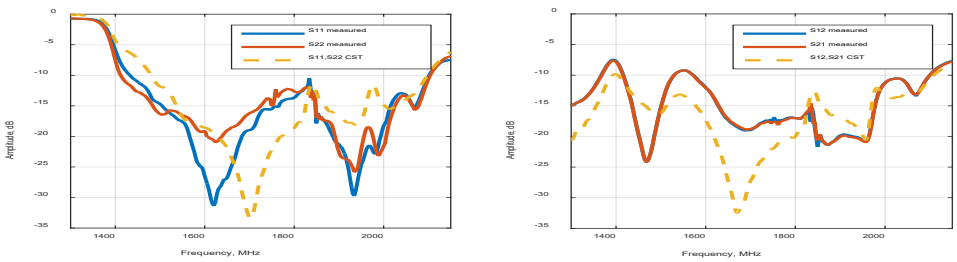

Fig. 5. The measured and predicted S parameters of feed horn. (Left) Return loss feed horn ports. (Right) Isolation between ports.

6. RECEIVER FRONT-END

Receiver front-end consists of two-channel low noise amplifiers (LNA), which are uncooled. LNAs are two-stage design optimized for the lowest noise figure at 1650 MHz. LNAs employ of-the-shelf MMIC device Skyworks SKY67151 for the first stage, and Mini-Circuits PGA103+ for the second stage. Input of LNAs contains microstrip directional couplers for calibration noise injection. While amplifiers are operated in the unregulated ambient environment, a calibration noise

source is positioned at the temperature regulated vertex room. Noise signal is fed via a separate coaxial cable through Wilkinson power divider to directional coupler inputs. Power supply voltage for amplifiers are provided through signal cables with the help of built-in bias-T circuits. To reduce degradation of noise temperature, short RG401 semi-rigid cables are used for connection between inputs of amplifiers and feed horn ports. Noise temperature of ≈30 K and gain of 32 dB was measured at 1650 MHz using Agilent 346A noise source. Results are shown in Fig. 7. Noticeable negative gain slope is equalized at intermediate frequency stages.

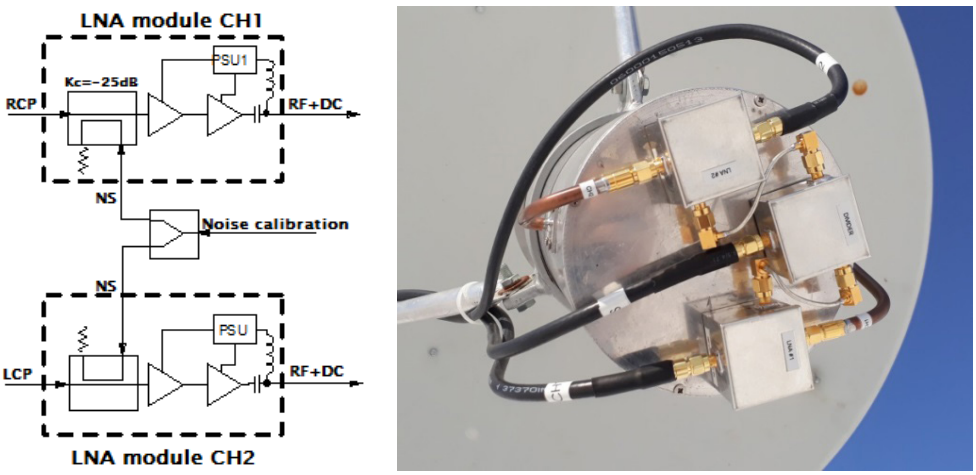

Fig. 6. Block diagram of receiver front-end and practical implementation. Amplifiers and calibration noise divider are positioned above the feed horn.

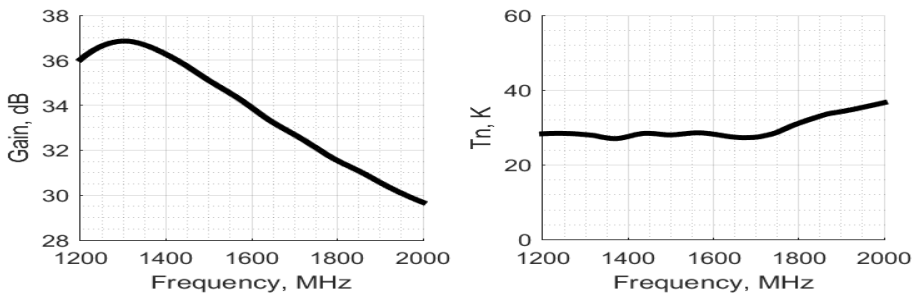

Fig. 7. Measured gain (left) and noise temperature (right) of L-band low noise amplifier. Measurement includes microstrip directional coupler at the amplifier input.

7. TELESCOPE SENSITIVITY

Sensitivity was evaluated in terms of system effective flux density (*SEFD*) by observing astronomical calibrator sources 3C123, 3C286 and 3C196 at various

antenna elevation positions. Standard "ON-OFF" procedure using frequency selective total power back-end was employed and *SEFD* calculated using (4):

$$SEFD = S_f \frac{P_{off}}{P_{on} - P_{off}} . \quad (4)$$

S_f is source flux density and T_{on}, T_{off} are total power values with beam pointing on and off source, respectively. Before *SEFD* measurement, beam pointing offsets were characterised and compensated by applying a pointing model, which was integrated in VLBI Field System software package. Weather conditions during measurement were excellent with clear sky and no wind. Result of measurement is showed in Fig. 8. As it can be seen, *SEFD* is 700 to 800 Jy within the typical operating elevation range between 20º and 60º.

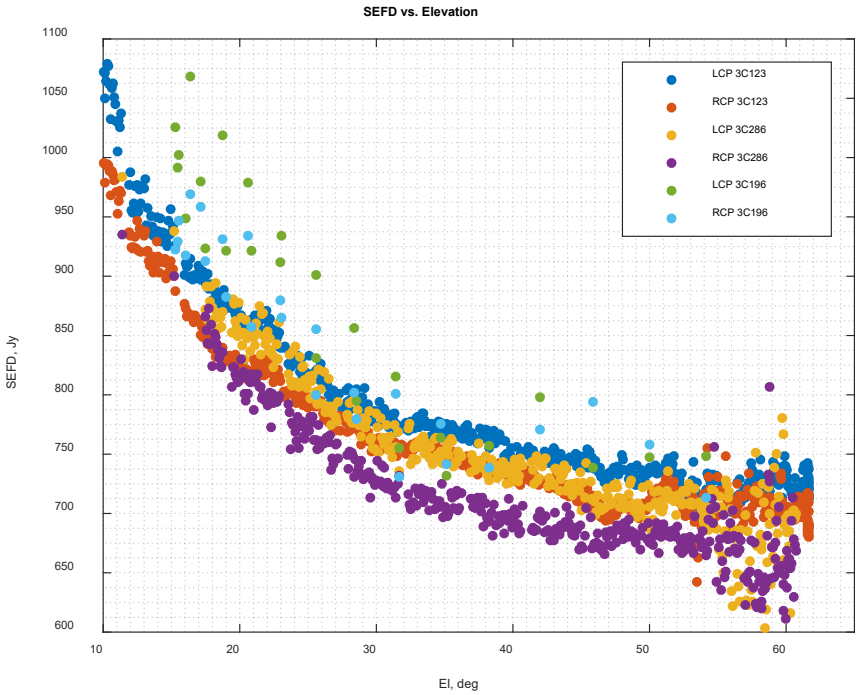

Fig. 8. Measured *SEFD* vs. elevation of RT-32 at 1650 MHz. Date of measurement: 6 April 2019.

SEFD is obtained by direct measurement and contains information about both the aperture efficiency and system noise temperature T_{sys}. To get an idea of actual aperture efficiency, absolute value of T_{sys} must be known. T_{sys} dependence on elevation was measured during *SEFD* measurement session and assuming injected calibration noise power was stable during relatively short measurement, relative characteristic shape of the measured T_{sys} curve should be accurate. To verify and compare absolute values of T_{sys} data, antenna noise temperature T_a was modelled using software described in [8], which rotates and integrates the antenna radiation

pattern in the elevation dependant noise environment. Full theta range radiation pattern version of Fig. 3 was used. Resulting T_{sys} is a sum of antenna and measured receiver noise temperatures ($T_n \approx 30$ K) and is shown in Fig. 9. Small correction to laboratory estimated injected calibration noise values used in T_{sys} measurements were applied using a simple constant scaling factor so that an absolute value of measured T_{sys} for both channels matches the theoretic curve. No correction to curve shape was applied as it already matched quite closely to the theoretic one. Obtained T_{sys} data together with *SEFD* measurements were used to calculate antenna aperture efficiency using (5):

$$e_A = 2k\frac{T_{sys}}{A_{phys}SEFD}10^{26}. \quad (5)$$

A_{phys} is a physical area of antenna, and k is Boltzmann constant. Resulting aperture efficiency is shown in left panel of Fig. 9. The obtained value of ≈ 26 % is 10 % less than the estimated one from physical optics simulation. Reason for this could be underestimated RT-32 surface and secondary mirror alignment efficiency factors or absolute values of T_{sys}. It should be mentioned that no influence of central C-band feed horn structure proximity (see Fig. 4) was modelled and should be investigated in future.

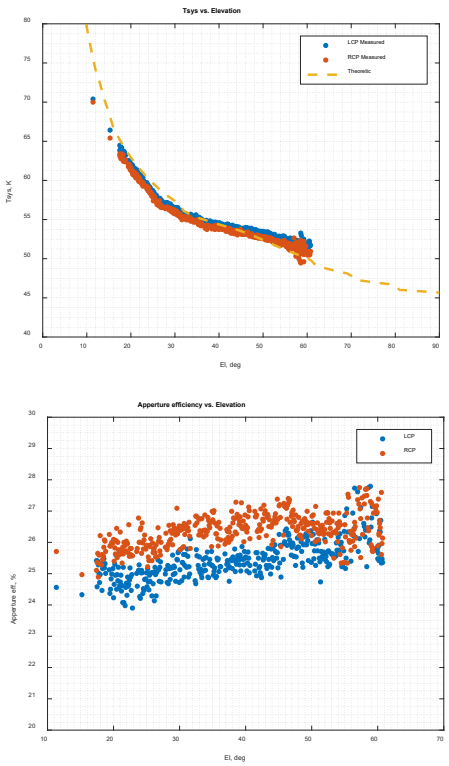

Fig. 9. (Left) The simulated and measured system noise temperature at 1650 MHz. (Right) The estimated aperture efficiency using data of Fig. 8 , Fig. 9 and (5). Data points were obtained from 3C286 calibrator observations.

8. THE FIRST OBSERVATION TESTS

Multiple astronomical observations were carried to test the receiver in single antenna and VLBI modes. Figure 10 shows the example of spectral line result obtained during single antenna mode tests. FFT spectrometer was used as registration backend in the frequency switching mode with spectral resolution of 0.38 KHz and integration time 80 seconds. Figure 11 highlights the result of EVN fringe test experiment FR057 at L-band. The obtained fringe amplitudes are comparable to other equivalent size antennas. Both results show acceptable isolation of cross-polarized channels.

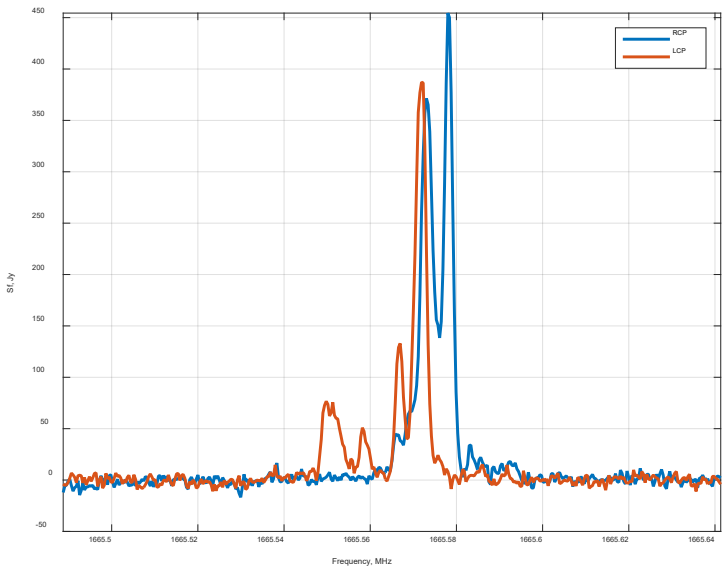

Fig. 10. Single antenna observation test result – spectral line towards W3(OH) at 1665 MHz. Total integration time: 80 s. Date of observation: 20 March 2019.

Vex file -- Integration time: 2s -- Start of the integration: 2019y023d14h20m00s0ms

FR057	Auto correlations						Cross correlations				
	Ef	Hh	Ir	O8	On	Tr	Ef-Hh	Ef-Ir	Ef-O8	Ef-On	Ef-Tr
1634.49MHz, LSB, Rcp-Rcp	1	1	1	1	1	1	276.2 A P offset: 0	634.8 A P offset: 0	895.6 A P offset: 3	838.4 A P offset: -1	1117 A P offset: 4
1634.49MHz, LSB, Rcp-Lcp	Cross hands						29.38 A P offset: 0	88.78 A P offset: 0	14.24 A P offset: 3	15.47 A P offset: 0	65.11 A P offset: 4
1634.49MHz, LSB, Lcp-Lcp	9	9	9	9	9	5	300.8 A P offset: 0	656.5 A P offset: 0	1062 A P offset: 3	870 A P offset: -1	776 A P offset: 4
1634.49MHz, LSB, Lcp-Rcp	Cross hands						15.92 A P offset: 0	149.9 A P offset: 0	60.64 A P offset: 3	65.15 A P offset: -1	187.5 A P offset: 4
1634.49MHz, USB, Rcp-Rcp	1	1	1	1	1	1	284.5 A P offset: 0	666 A P offset: 0	969.7 A P offset: -3	935 A P offset: 1	1070 A P offset: -4
1634.49MHz, USB, Rcp-Lcp	Cross hands						26.79 A P offset: 0	96.2 A P offset: 0	17.22 A P offset: -3	14.03 A P offset: 0	52.01 A P offset: -4
1634.49MHz, USB, Lcp-Lcp	9	9	9	9	9	5	260.8 A P offset: 0	628 A P offset: 0	1192 A P offset: -3	986 A P offset: 1	805 A P offset: -4
1634.49MHz, USB, Lcp-Rcp	Cross hands						13.58 A P offset: 0	134.4 A P offset: 0	67.9 A P offset: -3	68.6 A P offset: 1	215.2 A P offset: -4
1650.49MHz, LSB, Rcp-Rcp	2	2	2	2	2	2	297.5 A P offset: 0	654.2 A P offset: 0	1077 A P offset: 3	966.2 A P offset: -1	1070 A P offset: 4
1650.49MHz, LSB, Rcp-Lcp	Cross hands						23.99 A P offset: 0	79.23 A P offset: 0	16.69 A P offset: 3	11.53 A P offset: 0	56.11 A P offset: 4
1650.49MHz, LSB, Lcp-Lcp	10	10	10	10	10	6	249.2 A P offset: 0	657.1 A P offset: 0	1228 A P offset: 3	945.3 A P offset: -1	862.8 A P offset: 4

Fig. 11. First VLBI fringes using presented low-cost L-band receiver in EVN test observation FR057. Irbene RT-32 telescope designator is 'Ir'.

9. CONCLUSIONS

Low-cost L-band receiving system front-end intended for Irbene RT-32 Cassegrain radio telescope has been presented in the paper. Use of the third reflector significantly reduces feed antenna dimensions, hence, cost and complexly of manufacturing. Permanent installation at offset position reduces maintenance and frequency band switch-over time. Downside of this solution is reduced aperture efficiency due to diffraction losses of electrically small reflector and loss due to blocked aperture. In terms of system effective flux density, combined with uncooled low noise amplifiers, overall estimated telescope sensitivity is 700 to 800 Jy within usual elevation range, which corresponds to system noise temperature and aperture efficiency of ≈55 K and ≈26 %, respectively. The obtained sensitivity is average and could be improved 3 to 4 times if the appropriate full-size feed horn and cryogenic amplifiers are used, which already has been planned within ongoing RT-32 vertex room redesign project. Nevertheless, it has been proven by actual observations that performance of the presented system is sufficient to be useful as a temporal L-band receiver in various astronomy projects currently ongoing at VIRAC, including participation in EVN and observing relatively bright spectral lines in a single antenna mode.

ACKNOWLEDGEMENTS

The research has been funded by the Latvian Council of Science, project "Complex Investigations of the Small Bodies in the Solar System", No. lzp-2018/1-0401.

REFERENCES

1. Trokss, J., Lesins, A., Gaigals, G., Nechaeva, M., & Bezrukovs, Vl. (2013). Receiving system for ionosphere research. *Latvian Journal of Physics and Technical Sciences*, *49*(6), 13-17. DOI: 10.2478/v10047-012-0038-9
2. Bleiders, M., & Trokss, J. (2016). Development of receiver system for radio-astronomical observations at L band. *Space Research Review*, *4*, 77–84. ISBN 978-9984-648-64-4
3. Goldsmith, P. F. (1998). Quasioptical Systems: Gaussian Beam Quasioptical Propogation and Applications. *Wiley-IEEE Press*. ISBN: 978-0-7803-3439-7
4. Wylde, R. J. (1984). Millimetre-wave Gaussian beam-mode optics and corrugated feed horns. *IEE Proceedings, Part H - Microwaves, Optics and Antennas, 131*, 258–262. DOI: 10.1049/ip-h-1.1984.0053
5. Galuscak, R., Watanabe, M., Hazdra, P., Takeda, S., Seki, K., Prochazka, M., & Uchiyama, Y. (2008). Design of primary feeds for 32m KDDI antenna system IBA-4 in Cassegrain configuration. *Radio Engineering, 17(1)*. 20-27.
6. Galuscak, R., Hazdra, P. (2007). Prime-focus circular waveguide feed with septum polarization transformer, *DUBUS* 36(1), 8-32. ISSN: 1438-3705
7. Arias-Acuña, M., García-Pino, A., & Rubiños-López, O. (2013). Fast far field computation of single and dual reflector antennas. *Journal of Engineering, 2013*. DOI: 10.1155/2013/140254

8. Galuscak, R., Galuščáková, P., Mazanek, M., Hazdra, P., & Macas, M. (2009). Antenna Noise Temperature Calculator, *DUBUS* 3/2009. ISSN: 1438-3705

L DIAPAZONA UZTVEROŠĀS SISTĒMAS IEEJAS TRAKTS IRBENES RT-32 RADIOTELESKOPAM

M. Bleiders, A. Bērziņš, N. Jēkabsons,
K. Šķirmante, V. Bezrukovs

Kopsavilkums

Irbenes RT-32 radioteleskops ir viens no galvenajiem Ventspils Starptautiskā Centra (VSRC) instrumentiem, kas tiek izmantots VLBI un vienas antenas režīma novērojumos, tai skaitā dalībai Eiropas VLBI tīklā (EVN) un citos astronomijas projektos, piemēram, nesen uzsāktajā projektā "Kompleksie Saules sistēmas mazo ķermeņu pētījumi", kas saistās ar vāju spektrālo radiolīniju uztveršanu L diapazonā. Kopš darbības uzsākšanas, RT-32 ir pieejams C-X diapazona uztvērējs, bet regulāri tiek saņemts pieprasījums pēc novērojumiem L diapazona frekvencēs. RT-32 ģeometrijas gadījumā, optimālas veiktspējas iegūšanai L diapazonā ir nepieciešams ļoti liela izmēra apstarotājs, kura instalācija bez ievērojamas sekundārā fokusa konusa pārbūves ir sarežģīta. Kamēr šī pārbūve tiek veikta un tiek projektēts augstas veiktspējas apstarotājs, kā pagaidu risinājums ir izstrādāta kompakta uztverošā sistēma, kas ar sānisku nobīdi ir instalēta sekundārajā fokusā. Ņemto vērā ierobežoto izstrādes un izgatavošanas budžetu, iegūtā uztvērēja veiktspējā ir pietiekama lielai daļai šī brīža VSRC vajadzībām. Uztvērējs sastāv no maza izmēra paraboliskās antenas, kas ļauj izmantot kompaktu apstarotāju ar diviem cirkulāri polarizētiem kanāliem, tādējādi kopumā veidojot trīs spoguļu sistēmu. Ieejas trakta priekš pastiprinātāji netiek dzesēti, kas ļauj samazināt izgatavošanas un uzturēšanas izmaksas. Praktiski sistēmas testi parāda, ka iegūtā radio teleskopa jutība 1650 MHz frekvencē ir aptuveni 750 Jy. Šajā rakstā tiek izklāstīta uztvērēja galveno komponenšu izstrāde un sniegts svarīgāko parametru praktisks novērtējums.

30.05.2019.